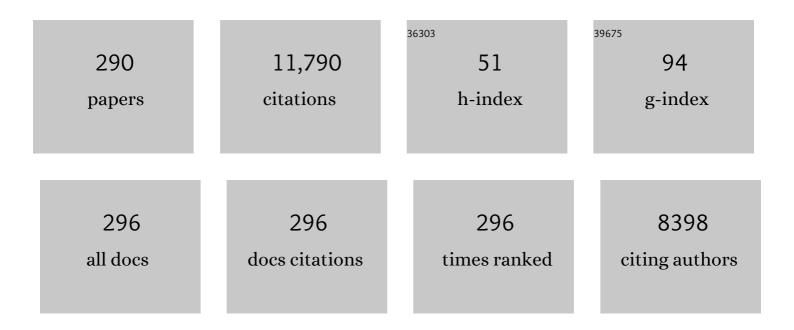
## Truls E Norby

List of Publications by Year in descending order

Source: https://exaly.com/author-pdf/7616618/publications.pdf Version: 2024-02-01



#	Article	IF	CITATIONS
1	Lanthanum strontium cobaltite as interconnect in oxide thermoelectric generators. Solid State Sciences, 2022, 124, 106801.	3.2	5
2	La2Ce2O7 doped with alkaline earth elements: Phase behavior, hydration and electrical properties. Journal of Alloys and Compounds, 2022, 899, 163306.	5.5	15
3	Impedance spectroscopy study of Au electrodes on Gd-doped CeO2 (GDC) – Molten Li2CO3+Na2CO3 (LNC) composite electrolytes. Journal of Power Sources, 2022, 522, 230986.	7.8	4
4	Immobilization of FeFe-hydrogenase on black TiO2 nanotubes as biocathodes for the hydrogen evolution reaction. Electrochemistry Communications, 2022, 135, 107221.	4.7	8
5	La1-xSrxMO3 (M = Co, Mn, Cr) interconnects in a 4-leg all-oxide thermoelectric generator at high temperatures. Journal of Physics and Chemistry of Solids, 2022, 167, 110739.	4.0	1
6	Single-step hydrogen production from NH <sub>3</sub> , CH <sub>4</sub> , and biogas in stacked proton ceramic reactors. Science, 2022, 376, 390-393.	12.6	56
7	Protonic Conduction in La <sub>2</sub> NiO <sub>4+</sub> <i><sub>δ</sub></i> and La <sub>2â€</sub> <i><sub>x</sub>A<sub>x</sub></i> NiO <sub>4+</sub> <i><sub>î´</sub></i> ( <i>A</i> Â= Ca,)	<b>⊺∌⊞</b> Qq1	⊉ <b>D</b> .78431
8	Quantifiable models for surface protonic conductivity in porous oxides – case of monoclinic ZrO <sub>2</sub> . Physical Chemistry Chemical Physics, 2022, 24, 11856-11871.	2.8	6
9	Mechanisms for sonochemical oxidation of nitrogen. Physical Chemistry Chemical Physics, 2022, 24, 15357-15364.	2.8	2
10	Galvanic Restructuring of Exsolved Nanoparticles for Plasmonic and Electrocatalytic Energy Conversion. Small, 2022, 18, .	10.0	2
11	High performance and toxicity assessment of Ta3N5 nanotubes for photoelectrochemical water splitting. Catalysis Today, 2021, 361, 57-62.	4.4	3
12	Photocatalytic generation of gas phase reactive oxygen species from adsorbed water: Remote action and electrochemical detection. Journal of Environmental Chemical Engineering, 2021, 9, 104809.	6.7	10
13	Increasing the thermal expansion of proton conducting Y-doped BaZrO3 by Sr and Ce substitution. Solid State Ionics, 2021, 359, 115534.	2.7	10
14	Enhanced activity of catalysts on substrates with surface protonic current in an electrical field – a review. Chemical Communications, 2021, 57, 5737-5749.	4.1	21
15	Near-Broken-Gap Alignment between FeWO <sub>4</sub> and Fe <sub>2</sub> WO <sub>6</sub> for Ohmic Direct p–n Junction Thermoelectrics. ACS Applied Materials & Interfaces, 2021, 13, 7416-7422.	8.0	11
16	Visible Light Driven Photocatalytic Decolorization and Disinfection of Water Employing Reduced TiO2 Nanopowders. Catalysts, 2021, 11, 228.	3.5	15
17	Al-doped ZnO prepared by co-precipitation method and its thermoelectric characteristics. Materials Letters, 2021, 288, 129352.	2.6	21
18	Versatile four-leg thermoelectric module test setup adapted to a commercial sample holder system for high temperatures and controlled atmospheres. Review of Scientific Instruments, 2021, 92, 043902.	1.3	3

#	Article	IF	CITATIONS
19	Double Perovskite Cobaltites Integrated in a Monolithic and Noble Metal-Free Photoelectrochemical Device for Efficient Water Splitting. ACS Applied Materials & Interfaces, 2021, 13, 20313-20325.	8.0	17
20	Development of Proton Conducting Ceramic Cells in Metal Supported Architecture. ECS Transactions, 2021, 103, 1779-1789.	0.5	3
21	Microstructure and electrochemical behavior of layered cathodes for molten carbonate fuel cell. Journal of Power Sources, 2021, 500, 229949.	7.8	11
22	Metal Supported Proton Conducting Ceramic Cell with Thin Film Electrolyte for Electrolysis Application. ECS Transactions, 2021, 103, 693-700.	0.5	0
23	Water Vapor Photoelectrolysis in a Solid-State Photoelectrochemical Cell with TiO <sub>2</sub> Nanotubes Loaded with CdS and CdSe Nanoparticles. ACS Applied Materials & Interfaces, 2021, 13, 46875-46885.	8.0	16
24	In situ cofactor regeneration enables selective CO2 reduction in a stable and efficient enzymatic photoelectrochemical cell. Applied Catalysis B: Environmental, 2021, 296, 120349.	20.2	21
25	Facet-engineered TiO <sub>2</sub> nanomaterials reveal the role of water–oxide interactions in surface protonic conduction. Journal of Materials Chemistry A, 2021, 10, 218-227.	10.3	8
26	Voids in walls of mesoporous TiO2 anatase nanotubes by controlled formation and annihilation of protonated titanium vacancies. Materials Chemistry and Physics, 2020, 239, 121953.	4.0	5
27	Thermoelectric properties of A-site deficient La-doped SrTiO3 at 100–900â€ <sup>–</sup> °C under reducing conditions. Journal of the European Ceramic Society, 2020, 40, 401-407.	5.7	32
28	Thermoelectric properties of non-stoichiometric CaMnO3-δ composites formed by redox-activated exsolution. Journal of the European Ceramic Society, 2020, 40, 1344-1351.	5.7	17
29	Structure and water uptake in BaLnCo2O6â~δ (Ln =La, Pr, Nd, Sm, Gd, Tb and Dy). Acta Materialia, 2020, 199, 297-310.	7.9	18
30	lonic conductivity in LixTaOy thin films grown by atomic layer deposition. Electrochimica Acta, 2020, 361, 137019.	5.2	6
31	Support effects on catalysis of low temperature methane steam reforming. RSC Advances, 2020, 10, 26418-26424.	3.6	14
32	Structure, hydration, and proton conductivity in 50% La and Nd doped CeO2 – La2Ce2O7 and Nd2Ce2O7 – and their solid solutions. Solid State Ionics, 2020, 354, 115401.	2.7	18
33	Defects and polaronic electron transport in Fe <sub>2</sub> WO <sub>6</sub> . Physical Chemistry Chemical Physics, 2020, 22, 15541-15548.	2.8	5
34	High-Temperature Structural and Electrical Properties of BaLnCo2O6 Positrodes. Materials, 2020, 13, 4044.	2.9	15
35	First-Principles Analyses of Nanoionic Effects at Oxide–Oxide Heterointerfaces for Electrochemical Applications. Journal of Physical Chemistry C, 2020, 124, 14072-14081.	3.1	1
36	Assessing common approximations in space charge modelling to estimate the proton resistance across grain boundaries in Y-doped BaZrO <sub>3</sub> . Physical Chemistry Chemical Physics, 2020, 22, 11891-11902.	2.8	7

#	Article	IF	CITATIONS
37	Disagreements between space charge models and grain boundary impedance data in yttrium-substituted barium zirconate. Solid State Ionics, 2020, 353, 115369.	2.7	13
38	Effects of metal cation doping in CeO <sub>2</sub> support on catalytic methane steam reforming at low temperature in an electric field. RSC Advances, 2020, 10, 14487-14492.	3.6	20
39	Importance of the Spin–Orbit Interaction for a Consistent Theoretical Description of Small Polarons in Pr-Doped CeO <sub>2</sub> . Journal of Physical Chemistry C, 2020, 124, 15831-15838.	3.1	9
40	Silver coated cathode for molten carbonate fuel cells. International Journal of Hydrogen Energy, 2020, 45, 19847-19857.	7.1	12
41	MOF-modified polyester fabric coated with reduced graphene oxide/polypyrrole as electrode for flexible supercapacitors. Electrochimica Acta, 2020, 336, 135743.	5.2	45
42	First observation of surface protonics on SrZrO <sub>3</sub> perovskite under a H <sub>2</sub> atmosphere. Chemical Communications, 2020, 56, 2699-2702.	4.1	13
43	Chemical stability of Ca <sub>3</sub> Co <sub>4â^'x</sub> O <sub>9+Î′</sub> /CaMnO <sub>3â^Î′</sub> p–n junction for oxide-based thermoelectric generators. RSC Advances, 2020, 10, 5026-5031.	3.6	3
44	Charge-Carrier Enrichment at BaZrO <sub>3</sub> /SrTiO <sub>3</sub> Interfaces. Journal of Physical Chemistry C, 2019, 123, 20808-20816.	3.1	7
45	Black Anatase TiO <sub>2</sub> Nanotubes with Tunable Orientation for High Performance Supercapacitors. Journal of Physical Chemistry C, 2019, 123, 21931-21940.	3.1	33
46	Composite Membranes for High Temperature PEM Fuel Cells and Electrolysers: A Critical Review. Membranes, 2019, 9, 83.	3.0	114
47	Investigation of the electrostatic potential of a grain boundary in Y-substituted BaZrO3 using inline electron holography. Physical Chemistry Chemical Physics, 2019, 21, 17662-17672.	2.8	10
48	Fabrication of Metal-Supported Proton-Conducting Electrolysers with Thin Film Sr- and Ce-Doped BZY Electrolyte. ECS Transactions, 2019, 91, 941-949.	0.5	3
49	Development of Metal Supported Cells Using BaZrO3-Based Proton Conducting Ceramics. ECS Transactions, 2019, 91, 1035-1045.	0.5	5
50	Surface reactivity and cation non-stoichiometry in BaZr <sub>1â^'x</sub> Y <sub>x</sub> O <sub>3â^'Î</sub> ( <i>x</i> = 0–0.2) exposed to CO <sub>2</sub> at elevated temperature. Journal of Materials Chemistry A, 2019, 7, 3848-3856.	10.3	21
51	Deep decarbonization efforts in Norway for energy sustainability. MRS Energy & Sustainability, 2019, 6, 1.	3.0	1
52	Acid reactions in hub systems consisting of separate non-reactive CO2 transport lines. International Journal of Greenhouse Gas Control, 2019, 87, 246-255.	4.6	17
53	Mixed proton and electron conducting double perovskite anodes for stable and efficient tubular proton ceramic electrolysers. Nature Materials, 2019, 18, 752-759.	27.5	191
54	Preparation of TiO2 rutile nanorods decorated with cobalt oxide nanoparticles for solar photoelectrochemical activity. Materials Letters, 2019, 247, 1-3.	2.6	8

#	Article	IF	CITATIONS
55	A textile-based wearable supercapacitor using reduced graphene oxide/polypyrrole composite. Electrochimica Acta, 2019, 305, 187-196.	5.2	125
56	Highly Correlated Hydride Ion Tracer Diffusion in SrTiO <sub>3–<i>x</i></sub> H <i><sub><i>x</i></sub></i> Oxyhydrides. Journal of the American Chemical Society, 2019, 141, 4653-4659.	13.7	20
57	Thermoelectric Properties of Ca3Co2â^'xMnxO6 (x = 0.05, 0.2, 0.5, 0.75, and 1). Materials, 2019, 12, 497.	2.9	6
58	Effect of SO2, O2, NO2, and H2O Concentrations on Chemical Reactions and Corrosion of Carbon Steel in Dense Phase CO2. Corrosion, 2019, 75, 1327-1338.	1.1	15
59	Improved CO2 flux by dissolution of oxide ions into the molten carbonate phase of dual-phase CO2 separation and Purification Technology, 2019, 212, 723-727.	7.9	10
60	Hydrogen from wet air and sunlight in a tandem photoelectrochemical cell. International Journal of Hydrogen Energy, 2019, 44, 587-593.	7.1	22
61	Ta3N5/Co(OH)x composites as photocatalysts for photoelectrochemical water splitting. Photochemical and Photobiological Sciences, 2019, 18, 837-844.	2.9	14
62	ls ReO <sub>3</sub> a mixed ionic–electronic conductor? A DFT study of defect formation and migration in a <i>B</i> <sup>VI</sup> O <sub>3</sub> perovskite-type oxide. Physical Chemistry Chemical Physics, 2018, 20, 8008-8015.	2.8	16
63	Chemical tracer diffusion of Sr and Co in polycrystalline Ca-deficient CaMnO <sub>3â^î^</sub> with CaMn <sub>2</sub> O <sub>4</sub> precipitates. Physical Chemistry Chemical Physics, 2018, 20, 2754-2760.	2.8	6
64	Protonic surface conduction controlled by space charge of intersecting grain boundaries in porous ceramics. Journal of Materials Chemistry A, 2018, 6, 8265-8270.	10.3	30
65	Inter-diffusion across a direct p-n heterojunction of Li-doped NiO and Al-doped ZnO. Solid State Ionics, 2018, 320, 215-220.	2.7	13
66	Performance and stability in H2S of SrFe0.75Mo0.25O3-δas electrode in proton ceramic fuel cells. Journal of the European Ceramic Society, 2018, 38, 163-171.	5.7	14
67	Evaluating surface protonic transport on cerium oxide via electrochemical impedance spectroscopy measurement. Solid State Communications, 2018, 270, 45-49.	1.9	29
68	Influence of processing on stability, microstructure and thermoelectric properties of Ca3Co4â^'xO9+δ. Journal of the European Ceramic Society, 2018, 38, 1592-1599.	5.7	25
69	Earth-Abundant Electrocatalysts in Proton Exchange Membrane Electrolyzers. Catalysts, 2018, 8, 657.	3.5	51
70	The influence of acceptor and donor doping on the protonic surface conduction of TiO <sub>2</sub> . Physical Chemistry Chemical Physics, 2018, 20, 15653-15660.	2.8	19
71	Ohmically heated ceramic asymmetric tubular membranes for gas separation. Journal of Membrane Science, 2018, 564, 598-604.	8.2	6
72	Intrinsic photoelectrocatalytic activity in oriented, photonic TiO2 nanotubes. Materials Science in Semiconductor Processing, 2018, 88, 186-191.	4.0	22

#	Article	IF	CITATIONS
73	All-Oxide Thermoelectric Module with in Situ Formed Non-Rectifying Complex p–p–n Junction and Transverse Thermoelectric Effect. ACS Omega, 2018, 3, 9899-9906.	3.5	13
74	Electrical Properties of a p–n Heterojunction of Li-Doped NiO and Al-Doped ZnO for Thermoelectrics. Journal of Electronic Materials, 2018, 47, 5296-5301.	2.2	6
75	Electrochemical and degradation study of Sr0.6Na0.4SiO3-δ. Journal of Solid State Electrochemistry, 2018, 22, 3009-3013.	2.5	2
76	Ba <sub>0.5</sub> Gd <sub>0.8</sub> La <sub>0.7</sub> Co <sub>2</sub> O <sub>6-î´</sub> Infiltrated in Porous BaZr <sub>0.7</sub> Ce <sub>0.2</sub> Y <sub>0.1</sub> O <sub>3</sub> Backbones as Electrode Material for Proton Ceramic Electrolytes. Journal of the Electrochemical Society, 2017, 164, F196-F202.	2.9	20
77	Thermal stability and enhanced thermoelectric properties of the tetragonal tungsten bronzes Nb8â^'xW9+xO47 (0 < x < 5). Journal of Materials Chemistry A, 2017, 5, 9768-9774.	10.3	17
78	Mechanisms of Protonic Surface Transport in Porous Oxides: Example of YSZ. Journal of Physical Chemistry C, 2017, 121, 12817-12825.	3.1	72
79	Comparison of Cu and Pt point-contact electrodes on proton conducting BaZr0.7Ce0.2Y0.1O3â^'. Solid State Ionics, 2017, 306, 38-47.	2.7	7
80	Layered microstructures based on BaZr0.85Y0.15O3â~'δ by pulsed laser deposition for metal-supported proton ceramic electrolyser cells. Journal of Materials Science, 2017, 52, 6486-6497.	3.7	17
81	Assessing the photoelectrochemical properties of C, N, F codoped TiO 2 nanotubes of different lengths. Catalysis Today, 2017, 287, 161-168.	4.4	31
82	Thermo-electrochemical production of compressed hydrogen from methane with near-zero energy loss. Nature Energy, 2017, 2, 923-931.	39.5	178
83	On the Conductivity of KBaPO4and Its Decomposition in Steam and Water. Journal of the Electrochemical Society, 2017, 164, F885-F888.	2.9	0
84	Relating defect chemistry and electronic transport in the double perovskite Ba <sub>1â^x</sub> Gd <sub>0.8</sub> La <sub>0.2+x</sub> Co <sub>2</sub> O <sub>6â^´Î</sub> (BGLC). Journal of Materials Chemistry A, 2017, 5, 15743-15751.	10.3	32
85	Electrochemical performance of Co3O4/CeO2 electrodes in H2S/H2O atmospheres in a proton-conducting ceramic symmetrical cell with BaZr0.7Ce0.2Y0.1O3 solid electrolyte. Solid State lonics, 2017, 306, 31-37.	2.7	9
86	Solid-state photoelectrochemical cell with TiO2 nanotubes for water splitting. Photochemical and Photobiological Sciences, 2017, 16, 10-16.	2.9	26
87	The Band Gap of BaPrO <sub>3</sub> Studied by Optical and Electrical Methods. Journal of the American Ceramic Society, 2016, 99, 492-498.	3.8	4
88	Surface defect chemistry of Y-substituted and hydrated BaZrO <sub>3</sub> with subsurface space-charge regions. Journal of Materials Chemistry A, 2016, 4, 7437-7444.	10.3	38
89	Solubility of transition metal interstitials in proton conducting BaZrO <sub>3</sub> and similar perovskite oxides. Journal of Materials Chemistry A, 2016, 4, 8105-8112.	10.3	44
90	Direct conversion of methane to aromatics in a catalytic co-ionic membrane reactor. Science, 2016, 353, 563-566.	12.6	341

#	Article	IF	CITATIONS
91	C-type related order in the defective fluorites La <sub>2</sub> Ce <sub>2</sub> O <sub>7</sub> and Nd <sub>2</sub> Ce <sub>2</sub> Ce <sub>2</sub> O <sub>7</sub> studied by neutron scattering and ab initio MD simulations. Physical Chemistry Chemical Physics, 2016, 18, 24070-24080.	2.8	18
92	Electrical characterization of amorphous LiAlO <sub>2</sub> thin films deposited by atomic layer deposition. RSC Advances, 2016, 6, 60479-60486.	3.6	34
93	Proton segregation and space-charge at the BaZrO3 (0 0 1)/MgO (0 0 1) heterointerface. Solid State Ionics, 2016, 297, 77-81.	2.7	11
94	Highlights from Faraday Discussion 182: Solid Oxide Electrolysis: Fuels and Feedstocks from Water and Air, York, UK, July 2015. Chemical Communications, 2016, 52, 1759-1767.	4.1	4
95	Reaction Kinetics of Protons and Oxide Ions in LSM/Lanthanum Tungstate Cathodes with Pt Nanoparticle Activation. Journal of the Electrochemical Society, 2016, 163, F507-F515.	2.9	16
96	On the development of proton ceramic fuel cells based on Ca-doped LaNbO4 as electrolyte. Journal of Power Sources, 2015, 282, 28-33.	7.8	45
97	Structural study of the complex perovskite Ba4(Ba2Nb2)O11. Materials Characterization, 2015, 102, 71-78.	4.4	3
98	Steam-promoted CO2 flux in dual-phase CO2 separation membranes. Journal of Membrane Science, 2015, 482, 115-119.	8.2	30
99	Tetragonal tungsten bronzes Nb <sub>8−x</sub> W <sub>9+x</sub> O <sub>47â^îŕ</sub> : optimization strategies and transport properties of a new n-type thermoelectric oxide. Materials Horizons, 2015, 2, 519-527.	12.2	15
100	Carbon Deposition and Sulfur Poisoning in SrFe <sub>0.75</sub> Mo <sub>0.25</sub> O <sub>3-δ</sub> and SrFe <sub>0.5</sub> Mn <sub>0.25</sub> Mo <sub>0.25</sub> O <sub>3-δ</sub> Electrode Materials for Symmetrical SOFCs. Journal of the Electrochemical Society, 2015, 162, F1078-F1087.	2.9	52
101	Hall effect measurements on thermoelectric Ca3Co4O9: On how to determine the charge carrier concentration in strongly correlated misfit cobaltites. Journal of Applied Physics, 2015, 117, .	2.5	10
102	Gd- and Pr-based double perovskite cobaltites as oxygen electrodes for proton ceramic fuel cells and electrolyser cells. Solid State Ionics, 2015, 278, 120-132.	2.7	136
103	Electromotive Force (emf) Determination of Transport Numbers for Native and Foreign Ions in Molten Alkali Metal Carbonates. Journal of the Electrochemical Society, 2015, 162, F1135-F1143.	2.9	23
104	Electrochemical promotion of the hydrogenation of CO 2 on Ru deposited on a BZY proton conductor. Journal of Catalysis, 2015, 331, 98-109.	6.2	44
105	Protons in Oxysulfides, Oxysulfates, and Sulfides: A First-Principles Study of La <sub>2</sub> O <sub>2</sub> S, La <sub>2</sub> O <sub>2</sub> SO <sub>SO<sub>4</sub>, SrZrS<sub>3</sub>, and BaZrS<sub>3</sub>. Journal of Physical Chemistry C, 2015, 119, 23875-23882.</sub>	3.1	23
106	Protons in piezoelectric langatate; La3Ga5.5Ta0.5O14. Solid State Ionics, 2015, 278, 275-280.	2.7	6
107	Versatile apparatus for thermoelectric characterization of oxides at high temperatures. Review of Scientific Instruments, 2014, 85, 103906.	1.3	31
108	Protons in acceptor doped langasite, La3Ga5SiO14. Solid State Ionics, 2014, 264, 76-84.	2.7	10

#	Article	IF	CITATIONS
109	Cathode compatibility, operation, and stability of LaNbO4-based proton conducting fuel cells. Solid State Ionics, 2014, 262, 382-387.	2.7	29
110	Cation transport in Sr and Cu substituted La2NiO4+δ studied by inter-diffusion. Solid State Ionics, 2014, 254, 32-39.	2.7	4
111	High temperature transport properties of thermoelectric CaMnO3â^'î′ — Indication of strongly interacting small polarons. Journal of Applied Physics, 2014, 115, 103705.	2.5	38
112	Electronic Transport Properties of [Ca <sub>2</sub> CoO <sub>3â^`δ</sub> ] <sub><i>q</i></sub> [CoO <sub>2</sub> ]. Journal of Physical Chemistry C, 2014, 118, 2908-2918.	3.1	39
113	Coking Study in Anode Materials for SOFCs: Physicochemical Properties and Behavior of Mo-Containing Perovskites in CO and CH <sub>4</sub> Fuels. ECS Transactions, 2014, 64, 103-116.	0.5	5
114	Oxygen Nonstoichiometry in (Ca <sub>2</sub> CoO <sub>3</sub> ) <sub>0.62</sub> (CoO <sub>2</sub> ): A Combined Experimental and Computational Study. Journal of Physical Chemistry C, 2014, 118, 18899-18907.	3.1	24
115	Hydrogen Oxidation Kinetics and Performance of Ni-LaNbO <sub>4</sub> Cermet Anodes for Proton Conducting SOFCs. Journal of the Electrochemical Society, 2014, 161, F373-F379.	2.9	6
116	Effects of temperature, triazole and hot-pressing on the performance of TiO2 photoanode in a solid-state photoelectrochemical cell. Electrochimica Acta, 2014, 115, 66-74.	5.2	10
117	Vacancy ordering and superstructure formation in dry and hydrated strontium tantalate perovskites: A TEM perspective. Micron, 2014, 62, 11-27.	2.2	4
118	Defect Chemistry of Rutile TiO <sub>2</sub> from First Principles Calculations. Journal of Physical Chemistry C, 2013, 117, 5919-5930.	3.1	45
119	The defect chemistry of nitrogen in oxides: A review of experimental and theoretical studies. Journal of Solid State Chemistry, 2013, 198, 65-76.	2.9	10
120	Inter-diffusion in lanthanum tungsten oxide. Solid State Ionics, 2013, 244, 57-62.	2.7	14
121	Solid Proton Conductors: Oxides and Polymers. Fuel Cells, 2013, 13, 4-5.	2.4	Ο
122	On the Complex Structural Picture of the Ionic Conductor Sr <sub>6</sub> Ta <sub>2</sub> O <sub>11</sub> . Journal of Physical Chemistry C, 2013, 117, 9543-9549.	3.1	6
123	Hydration of lanthanum tungstate (La/W=5.6 and 5.3) studied by TG and simultaneous TG–DSC. Solid State Ionics, 2013, 231, 25-29.	2.7	35
124	Solid-state photoelectrochemical H2 generation with gaseous reactants. Electrochimica Acta, 2013, 97, 320-325.	5.2	32
125	Determination of inter-diffusion coefficients for the A- and B-site in the A2BO4+ $\hat{I}$ (A = La, Nd and B = Ni,) Tj ETQq1	1 0.7843 2.7	14 rgBT /0 14
126	Determination of Chemical Tracer Diffusion Coefficients for the <scp><scp>La</scp></scp> ―and <scp><scp>Ni</scp></scp> â€site in <scp><scp>La</scp></scp> <sub>2</sub> <scp><scp>NiO</scp>4+δ Studied by <scp>SIMS</scp>. Journal of the American Ceramic Society, 2013, 96, 598-605.</scp>	3.8	9

#	Article	IF	CITATIONS
127	Investigation of La1â^'xSrxCrO3â^'â^, (x ~ 0.1) as Membrane for Hydrogen Production. Membranes, 2012, 2, 665-686.	3.0	23
128	Theoretical analysis of oxygen vacancies in layered sodium cobaltate, Na <sub><i>x</i></sub> CoO <sub>2â^îî</sub> . Journal of Physics Condensed Matter, 2012, 24, 475505.	1.8	15
129	Complete structural model for lanthanum tungstate: a chemically stable high temperature proton conductor by means of intrinsic defects. Journal of Materials Chemistry, 2012, 22, 1762-1764.	6.7	91
130	Nitrogen defects in wide band gap oxides: defect equilibria and electronic structure from first principles calculations. Physical Chemistry Chemical Physics, 2012, 14, 11808.	2.8	15
131	Interfacial Charge Transfer and Chemical Bonding in a Ni–LaNbO <sub>4</sub> Cermet for Proton-Conducting Solid-Oxide Fuel Cell Anodes. Chemistry of Materials, 2012, 24, 4152-4159.	6.7	16
132	H and Li Related Defects in ZnO and Their Effect on Electrical Properties. Journal of Physical Chemistry C, 2012, 116, 23764-23772.	3.1	33
133	Crystal structure, hydration and ionic conductivity of the inherently oxygen-deficient La2Ce2O7. Solid State Ionics, 2012, 228, 1-7.	2.7	77
134	Conductivity and hydration trends in disordered fluorite and pyrochlore oxides: A study on lanthanum cerate–zirconate based compounds. Solid State Ionics, 2012, 229, 26-32.	2.7	32
135	Hydration and proton conductivity in LaAsO <sub>4</sub> . Journal of Materials Chemistry, 2012, 22, 1652-1661.	6.7	29
136	Determination of the Self-Diffusion Coefficient of Ni2+in La2NiO4+Îby the Solid State Reaction Method. Journal of the Electrochemical Society, 2012, 159, B702-B708.	2.9	7
137	Kinetic Decomposition of a La2NiO4+ÎMembrane under an Oxygen Potential Gradient. Journal of the Electrochemical Society, 2012, 159, F461-F467.	2.9	3
138	Effects of A and B site acceptor doping on hydration and proton mobility of LaNbO4. International Journal of Hydrogen Energy, 2012, 37, 8004-8016.	7.1	55
139	Influence of Pr substitution on defects, transport, and grain boundary properties of acceptor-doped BaZrO3. International Journal of Hydrogen Energy, 2012, 37, 7962-7969.	7.1	21
140	Hydrogen energetics and charge transfer in the Ni/LaNbO4 interface from DFT calculations. International Journal of Hydrogen Energy, 2012, 37, 8033-8042.	7.1	6
141	Defect structure and its nomenclature for mixed conducting lanthanum tungstates La28–xW4+xO54+3x/2. International Journal of Hydrogen Energy, 2012, 37, 8051-8055.	7.1	66
142	On the hydration of grain boundaries and bulk of proton conducting BaZr0.7Pr0.2Y0.1O3-δ. International Journal of Hydrogen Energy, 2012, 37, 7970-7974.	7.1	5
143	Effect of cation disorder on the solubility and result of doping in oxides. International Journal of Hydrogen Energy, 2012, 37, 8062-8065.	7.1	3
144	Defects at the (1 1 0) surface of rutile TiO2 from ab initio calculations. International Journal of Hydrogen Energy, 2012, 37, 8110-8117.	7.1	13

#	Article	IF	CITATIONS
145	Atomistic study of LaNbO4; surface properties and hydrogen adsorption. International Journal of Hydrogen Energy, 2012, 37, 6674-6685.	7.1	13
146	Preface of the Special Issue of International Journal of Hydrogen Energy: Proceedings of the 7th Petite Workshop on the Defect Chemical Nature of Energy Materials. International Journal of Hydrogen Energy, 2012, 37, 7953.	7.1	0
147	Synthesis, Sintering, Transport Properties, and Surface Exchange of <scp><scp>La</scp></scp> <sub>2</sub> <scp><iscp>Ni</iscp></scp> 0.9 <scp>Cu</scp> Journal of the American Ceramic Society, 2012, 95, 2065-2073.	cb> <b>3°8</b> np>	0.1₄/sub> <sc< td=""></sc<>
148	One-dimensional WO3 and its hydrate: One-step synthesis, structural and spectroscopic characterization. Journal of Solid State Chemistry, 2012, 185, 245-252.	2.9	17
149	Neutron diffraction study of the monoclinic to tetragonal structural transition in LaNbO4 and its relation to proton mobility. Journal of Solid State Chemistry, 2012, 187, 27-34.	2.9	40
150	Nitrogen defects from NH <sub>3</sub> in rare-earth sesquioxides and ZrO <sub>2</sub> . Dalton Transactions, 2011, 40, 132-135.	3.3	9
151	Investigation of pitting resistance of titanium based on a modified point defect model. Corrosion Science, 2011, 53, 815-821.	6.6	70
152	Structure, Water Uptake, and Electrical Conductivity of TiP2O7. Journal of the American Ceramic Society, 2011, 94, 1514-1522.	3.8	46
153	Structure, chemical stability and mixed proton–electron conductivity in BaZr0.9â^xPrxGd0.1O3â^î^. Journal of Power Sources, 2011, 196, 9141-9147.	7.8	35
154	NdHO, a novel oxyhydride. Journal of Solid State Chemistry, 2011, 184, 1890-1894.	2.9	32
155	Microstructural characterization and electrical properties of spray pyrolyzed conventionally sintered or hot-pressed BaZrO3 and BaZr0.9Y0.1O3â^Î. Solid State Ionics, 2011, 182, 32-40.	2.7	41
156	Development of Proton Conducting SOFCs Based on LaNbO <sub>4</sub> Electrolyte – Status in Norway. Fuel Cells, 2011, 11, 17-25.	2.4	63
157	XPS characterisation of in situ treated lanthanum oxide and hydroxide using tailored charge referencing and peak fitting procedures. Journal of Electron Spectroscopy and Related Phenomena, 2011, 184, 399-409.	1.7	449
158	Oxygen bulk diffusion and surface exchange in Sr-substituted La2NiO4+δ. Solid State Ionics, 2011, 184, 42-46.	2.7	31
159	Proton Conductivity in Acceptor-Doped LaVO4. Journal of the Electrochemical Society, 2011, 158, B857.	2.9	22
160	Electron Microscopy Study of interfaces of Proton Conducting Fuel Cell Anodes. Microscopy and Microanalysis, 2010, 16, 1444-1445.	0.4	0
161	A Kr ¶ger-Vink Compatible Notation for Defects in Inherently Defective Sublattices. Journal of the Korean Ceramic Society, 2010, 47, 19-25.	2.3	50
162	Correlation between the characteristic green emissions and specific defects of ZnO. Physical Chemistry Chemical Physics, 2010, 12, 2373.	2.8	57

#	Article	IF	CITATIONS
163	Charge carriers in grain boundaries of 0.5% Sr-doped LaNbO4. Solid State Ionics, 2010, 181, 104-109.	2.7	61
164	Determination of the enthalpy of hydration of oxygen vacancies in Y-doped BaZrO3 and BaCeO3 by TG-DSC. Solid State Ionics, 2010, 181, 1740-1745.	2.7	55
165	A combined conductivity and DFT study of protons in PbZrO3 and alkaline earth zirconate perovskites. Solid State Ionics, 2010, 181, 130-137.	2.7	57
166	Space–charge theory applied to the grain boundary impedance of proton conducting BaZr0.9Y0.1O3â^Îr. Solid State Ionics, 2010, 181, 268-275.	2.7	219
167	High-temperature proton conductivity and defect structure of TiP2O7. Solid State Ionics, 2010, 181, 510-516.	2.7	49
168	Defects and transport properties of Sr-doped LaP3O9. Solid State Ionics, 2010, 181, 1264-1269.	2.7	8
169	XPS characterisation of the interface between anode and electrolyte in a proton conducting solid oxide fuel cell. Surface and Interface Analysis, 2010, 42, 568-571.	1.8	13
170	Novel Fabrication of Caâ€Doped LaNbO <sub>4</sub> Thinâ€Film Protonâ€Conducting Fuel Cells by Pulsed Laser Deposition. Journal of the American Ceramic Society, 2010, 93, 1874-1878.	3.8	10
171	Correlation of oxygen vacancy concentration and thermoelectric properties in Na0.73CoO2â^î´. Applied Physics Letters, 2010, 96, 141905.	3.3	30
172	Concentration and Mobility of Electrons in ZnO from Electrical Conductivity and Thermoelectric Power in H <sub>2</sub> + H <sub>2</sub> O at High Temperatures. Journal of Physical Chemistry C, 2010, 114, 16785-16792.	3.1	8
173	Hydration of Rutile TiO <sub>2</sub> : Thermodynamics and Effects on <i>n</i> - and <i>p</i> -Type Electronic Conduction. Journal of Physical Chemistry C, 2010, 114, 9139-9145.	3.1	25
174	Reactivity between Titanium Dioxide and Water at Elevated Temperatures. Journal of Physical Chemistry C, 2010, 114, 18215-18221.	3.1	21
175	Evaluation of metastable pitting on titanium by charge integration of current transients. Corrosion Science, 2010, 52, 3158-3161.	6.6	18
176	Preparation and Characterization of Ni–LaNbO <sub>4</sub> Cermet Anode Supports for Proton onducting Fuel Cell Applications. Journal of the American Ceramic Society, 2010, 93, 2650-2655.	3.8	23
177	High Temperature Proton Conductivity of ZrP[sub 2]O[sub 7]. Journal of the Electrochemical Society, 2010, 157, B1491.	2.9	15
178	Titanium Dioxide Photocatalyst - Unresolved Problems. Solid State Phenomena, 2010, 162, 77-90.	0.3	5
179	Ab initio studies of hydrogen and acceptor defects in rutile TiO2. Physical Chemistry Chemical Physics, 2010, 12, 6817.	2.8	30
180	Proton mobility through a second order phase transition: theoretical and experimental study of LaNbO4. Physical Chemistry Chemical Physics, 2010, 12, 10313.	2.8	66

Truls E Norby

#	Article	IF	CITATIONS
181	Transport properties and defect analysis of La1.9Sr0.1NiO4+δ. Solid State Ionics, 2009, 180, 1433-1441.	2.7	23
182	Defects and transport in Gd-doped BaPrO3. Journal of Electroceramics, 2009, 23, 80-88.	2.0	25
183	Structure, defect chemistry, and proton conductivity in nominally Sr-doped Ba3La(PO4)3. Solid State Ionics, 2009, 180, 338-342.	2.7	10
184	Conductivity and water uptake of Sr4(Sr2Nb2)O11·nH2O and Sr4(Sr2Ta2)O11·nH2O. Solid State Ionics, 2009, 180, 1151-1156.	2.7	32
185	Novel high temperature proton conducting fuel cells: Production of La0.995Sr0.005NbO4â^î^ electrolyte thin films and compatible cathode architectures. Journal of Power Sources, 2009, 188, 106-113.	7.8	31
186	Proton Conductivity in Perovskite Oxides. Fuel Cells and Hydrogen Energy, 2009, , 217-241.	0.6	30
187	Proton Conduction in Solids: Bulk and Interfaces. MRS Bulletin, 2009, 34, 923-928.	3.5	69
188	In situ studies of structural stability and proton conductivity of titanate nanotubes. Energy and Environmental Science, 2009, 2, 517.	30.8	19
189	High-Temperature Hydration and Conductivity of Mayenite, Ca <sub>12</sub> Al <sub>14</sub> O <sub>33</sub> . Journal of Physical Chemistry C, 2009, 113, 8938-8944.	3.1	31
190	Structural transitions and conductivity of BaPrO3 and BaPr0.9Y0.1O3â^'δ. Journal of Materials Chemistry, 2009, 19, 3238.	6.7	22
191	Local condensation around oxygen vacancies in t-LaNbO4 from first principles calculations. Physical Chemistry Chemical Physics, 2009, 11, 5550.	2.8	24
192	Steady-State Permeation of Oxygen Through La[sub 1.9]Sr[sub 0.1]NiO[sub 4+Î]. Journal of the Electrochemical Society, 2009, 156, B1039.	2.9	13
193	Structural study of the perovskite system Ba6â^'yCayNb2O11 hydrated to proton conducting Ba6â^'yCayNb2O10(OH)2. Solid State Ionics, 2008, 179, 1858-1866.	2.7	11
194	Effect of oxygen partial pressure on the oxidation behaviour of an yttria dispersion strengthened NiCr-base alloy. Journal of Materials Science, 2008, 43, 5591-5598.	3.7	16
195	An experimental study of the electronic structure of anodically grown films on an amorphous Ni <sub>78</sub> Si <sub>8</sub> B <sub>14</sub> alloy. Surface and Interface Analysis, 2008, 40, 826-829.	1.8	9
196	Oxygen and Hydrogen Separation Membranes Based on Dense Ceramic Conductors. Membrane Science and Technology, 2008, , 401-458.	0.5	29
197	High-Temperature Proton-Conducting Lanthanum Ortho-Niobate-Based Materials. Part II: Sintering Properties and Solubility of Alkaline Earth Oxides. Journal of the American Ceramic Society, 2008, 91, 879-886.	3.8	66
198	Protective and non-protective scale formation of NiCr alloys in water vapour containing high- and low-pO2 gases. Corrosion Science, 2008, 50, 1753-1760.	6.6	75

#	Article	IF	CITATIONS
199	Proton and oxide ion conductivity in grain boundaries and grain interior of Ca-doped Er2Ti2O7 with Si-impurities. Solid State Ionics, 2008, 179, 1849-1853.	2.7	18
200	A Study of Anodically Grown Hydroxide Films on an Amorphous Ni[sub 78]Si[sub 8]B[sub 14] Alloy. Journal of the Electrochemical Society, 2007, 154, F111.	2.9	8
201	Ceramic Proton and Mixed Proton-Electron Conductors in Membranes for Energy Conversion Applications. Journal of Chemical Engineering of Japan, 2007, 40, 1166-1171.	0.6	26
202	Mixed Ionic and Electronic Conductivity of Undoped and Acceptor-Doped Er[sub 6]WO[sub 12]. Journal of the Electrochemical Society, 2007, 154, B77.	2.9	31
203	Role of protons in the electrical conductivity of acceptor-doped BaPrO3, BaTbO3, and BaThO3. Solid State Ionics, 2007, 178, 461-467.	2.7	36
204	Synthesis, densification and electrical properties of strontium cerate ceramics. Journal of the European Ceramic Society, 2007, 27, 4461-4471.	5.7	29
205	High-Temperature Proton Conductivity in Acceptor-Substituted Rare-Earth Ortho-Tantalates, LnTaO4. Journal of the American Ceramic Society, 2007, 90, 1116-1121.	3.8	64
206	Dense ceramic membranes based on ion conducting oxides. Annales De Chimie: Science Des Materiaux, 2007, 32, 197-212.	0.4	25
207	Novel anode materials for multi-fuel applicable solid oxide fuel cells. Journal of Alloys and Compounds, 2006, 408-412, 622-627.	5.5	13
208	Dense Ceramic Membranes for Hydrogen Separation. , 2006, , 1-48.		18
209	Electron Probe Micro Analysis of A-Site Inter-Diffusion Between LaFeO3 and NdFeO3. Journal of the American Ceramic Society, 2006, 89, 582-586.	3.8	20
210	Proton conduction in rare-earth ortho-niobates and ortho-tantalates. Nature Materials, 2006, 5, 193-196.	27.5	457
211	Transport of hydrogen species in a single crystal SrTiO3. Solid State Ionics, 2006, 177, 1469-1476.	2.7	18
212	Cation self-diffusion in LaFeO3 measured by the solid state reaction method. Solid State Ionics, 2006, 177, 639-646.	2.7	53
213	High-temperature proton conductivity in acceptor-doped LaNbO4. Solid State Ionics, 2006, 177, 1129-1135.	2.7	160
214	Ionic and Electronic Conductivity of 5% Ca-Doped GdNbO[sub 4]. Journal of the Electrochemical Society, 2006, 153, J87.	2.9	21
215	On the Steady-State Oxygen Permeation Through La[sub 2]NiO[sub 4+Î] Membranes. Journal of the Electrochemical Society, 2006, 153, A233.	2.9	72
216	PROTONIC CONDUCTION IN <font>TiP</font> <sub>2</sub> <font>O</font> <sub>7</sub> ., 2006, .		0

#	Article	IF	CITATIONS
217	Entropy of oxidation and redox energetics of CaMnO. Solid State Ionics, 2005, 176, 2261-2267.	2.7	35
218	Protonic conduction in acceptor-doped LaP3O9. Solid State Ionics, 2005, 176, 2867-2870.	2.7	37
219	Proton conductivity of Ca-doped Tb2O3. Solid State Ionics, 2005, 176, 2957-2961.	2.7	22
220	Nonstoichiometry and reductive decomposition of CaMnO. Solid State Ionics, 2005, 176, 217-223.	2.7	79
221	Development of a hydrogen membrane reformer based CO2 emission free gas fired power plant. , 2005, , 83-91.		9
222	Conductivity dependence on oxygen partial pressure and transport number measurements of La2Mo2O9. Materials Research Society Symposia Proceedings, 2004, 822, S6.5.1.	0.1	0
223	Redox energetics of SrFeO3â^lr´â€" a coulometric titration study. Solid State Ionics, 2004, 167, 367-377.	2.7	40
224	Temperature dependence of oxygen ion transport in Sr+Mg-substituted LaGaO (LSGM) with varying grain sizes. Solid State Ionics, 2004, 174, 233-243.	2.7	51
225	Conductivity Dependence on Oxygen Partial Pressure and Oxide-Ion Transport Numbers Determination for La[sub 2]Mo[sub 2]O[sub 9]. Electrochemical and Solid-State Letters, 2004, 7, A373.	2.2	32
226	Oxidation Behavior of Ferritic Stainless Steels under SOFC Interconnect Exposure Conditions. Journal of the Electrochemical Society, 2004, 151, B669.	2.9	158
227	Hydrogen in oxides. Dalton Transactions, 2004, , 3012-3018.	3.3	342
228	Transport numbers from hydrogen concentration cells over different oxides under oxidising and reducing conditions. Dalton Transactions, 2004, , 3147.	3.3	16
229	Synthesis and characterisation of Ni–SrCe0.9Yb0.1O3â^'δ cermet anodes for protonic ceramic fuel cells. Solid State Ionics, 2003, 158, 333-342.	2.7	44
230	Impedance spectroscopy and proton transport number measurements on Sr-substituted LaPO4 prepared by combustion synthesis. Solid State Ionics, 2003, 162-163, 167-173.	2.7	54
231	grossly non-stoichiometric oxidesElectronic supplementary information (ESI) available: the experimental molar heat capacities of SrFeO2.54, SrFeO2.725 and SrFeO2.833 at sub-ambient temperatures and the corresponding data for SrFeO2.50, SrFeO2.74, SrFeO2.82, SrFeO2.833 and SrFeO2.85 at super-ambient temperatures. See http://www.rsc.org/suppdata/dt/b2/b209236k/. Dalton	3.3	16
232	Transactions, 2003, , 361-368. HT Corrosion of a Cr-5 wt % Fe-1 wt % Y[sub 2]O[sub 3] Alloy and Conductivity of the Oxide Scale. Journal of the Electrochemical Society, 2003, 150, B374.	2.9	33
233	Formation of YSZ Films By Thermal Annealing of Y/Zr Layers in Air. Surface Engineering, 2003, 19, 379-383.	2.2	4
234	Redox energetics of perovskite-related oxides. Journal of Materials Chemistry, 2002, 12, 317-323.	6.7	48

#	Article	IF	CITATIONS
235	Water and protons in electrodeposited MnO2 (EMD). Solid State Ionics, 2002, 152-153, 695-701.	2.7	10
236	XPS surface analyses of LaPO4ceramics prepared by precipitation with or without excess of PO43â^'. Surface and Interface Analysis, 2002, 34, 306-310.	1.8	37
237	Proton and apparent hydride ion conduction in Al-substituted SrTiO3. Solid State Ionics, 2002, 154-155, 669-677.	2.7	31
238	Fast oxygen ion conductors—from doped to ordered systems. Journal of Materials Chemistry, 2001, 11, 11-18.	6.7	65
239	High-temperature oxidation of Cu–30 wt.% Ni–15 wt.% Fe. Corrosion Science, 2001, 43, 283-299.	6.6	38
240	H <sub>2</sub> O-D <sub>2</sub> O exchange in lawsonite. American Mineralogist, 2001, 86, 1166-1169.	1.9	15
241	Hydrogen ion conduction in iron-substituted strontium titanate, SrTi1â^'xFexO3â^'x/2 (0≤â‰9.8). Solid State Ionics, 2001, 143, 103-116.	2.7	65
242	Incorporation of water in strontium tantalates with perovskite-related structure. Solid State Ionics, 2001, 145, 357-364.	2.7	31
243	The promise of protonics. Nature, 2001, 410, 877-878.	27.8	253
244	Segregation of Sr in Sr-doped LaPO4 ceramics. Surface and Interface Analysis, 2000, 30, 95-97.	1.8	22
245	Mixed hydrogen ion–electronic conductors for hydrogen permeable membranes. Solid State Ionics, 2000, 136-137, 139-148.	2.7	125
246	On phase relations, transport properties and defect structure in mixed conducting SrFe1.5â^'xCoxOz. Solid State Ionics, 2000, 129, 285-297.	2.7	23
247	Measurements of surface exchange kinetics and chemical diffusion in dense oxygen selective membranes. Catalysis Today, 2000, 56, 315-324.	4.4	22
248	Phase relations, chemical diffusion and electrical conductivity in pure and doped Sr4Fe6O13 mixed conductor materials. Solid State Ionics, 2000, 135, 687-697.	2.7	33
249	Spinel and Perovskite Functional Layers Between Plansee Metallic Interconnect (Cr-5 wt % Fe-1 wt %) Tj ETQq1 1 Solid Oxide Fuel Cells. Journal of the Electrochemical Society, 2000, 147, 3251.	0.784314 2.9	rgBT /Over 172
250	Protons and other defects in BaCeO3: a computational study. Solid State Ionics, 1999, 122, 145-156.	2.7	133
251	Solid-state protonic conductors: principles, properties, progress and prospects. Solid State Ionics, 1999, 125, 1-11.	2.7	747
252	Protons in Sr3(Sr1+xNb2a^'x)O9a^'3x/2 perovskite. Solid State Ionics, 1999, 125, 369-376.	2.7	45

#	Article	IF	CITATIONS
253	Title is missing!. Oxidation of Metals, 1999, 51, 221-233.	2.1	81
254	Ionic and electronic conductivity in CaTi1â^'xFexO3â^'δ (x=0.1–0.3). Ionics, 1999, 5, 385-392.	2.4	32
255	Defects and transport in SrFe1â^'xCoxO3â^'δ. Ionics, 1999, 5, 434-443.	2.4	40
256	Crystal Structure of the Mixed Oxides La0.7Sr0.3Co1â^'zMnzO3±y(0â‰ <b>z</b> â‰⊉). Journal of Solid State Chemistry, 1999, 143, 52-57.	2.9	29
257	Determination of Thermodynamics and Kinetics of Point Defects in Cu2 O  Using the Rosenburg Method Journal of the Electrochemical Society, 1999, 146, 999-1004.	<sup>•</sup> 2.9	29
258	lonic and electronic conductivity in CaTi <sub>0.9</sub> fe <sub>0.1</sub> o <sub>3-δ</sub> . Phase Transitions, 1999, 69, 157-168.	1.3	12
259	In Memory Per Kofstad. Oxidation of Metals, 1998, 49, 401-402.	2.1	0
260	Determination of thermodynamics and kinetics of point defects in NiO using the Rosenburg method. Solid State Ionics, 1998, 111, 323-332.	2.7	25
261	La1 â~' x Ba x Cr1 â~' y Ti y  O 3 with Varied Oxygen Content. Journal of the Electrochei 264-269.	mical Soci	iety, 1998, 12
262	Protonic and Native Conduction in Srâ€Substituted LaPO4 Studied by Thermoelectric Power Measurements. Journal of the Electrochemical Society, 1998, 145, 3313-3319.	2.9	77
263	High Temperature Proton Conductors. , 1998, , 603-608.		0
264	Concentration and transport of protons in oxides. Current Opinion in Solid State and Materials Science, 1997, 2, 593-599.	11.5	156
265	The equilibrium between water vapour, protons, and oxygen vacancies in rare earth oxides. Solid State Ionics, 1997, 97, 523-528.	2.7	48
266	THE DEFECT STRUCTUFE OF SrTi 1â^'x Fe x O 3â^'y ( x = 0–0.8) INVESTIGATED BY ELECTRICAL CONDUCTIVITY MEASUREMENTS AND ELECTRON ENERGY LOSS SPECTROSCOPY (EELS). Journal of Physics and Chemistry of Solids, 1997, 58, 969-976.	4.0	319
267	Studies of chemical diffusion in La <sub>1-X</sub> Sr <sub>X</sub> CoO <sub>3-Î</sub> . Phase Transitions, 1996, 58, 145-157.	1.3	7
268	Oxidation of methane on a Au + SrFeO3â^î///YSZ electrode characterised by mass spectroscopy and18O2 pulses. Chemical Engineering and Technology, 1995, 18, 139-147.	1.5	2
269	Proton and deuteron conductivity in CsHSO4 and CsDSO4 by in situ isotopic exchange. Solid State lonics, 1995, 77, 105-110.	2.7	84
270	Protons in rare earth oxides. Solid State Ionics, 1995, 77, 147-151.	2.7	74

#	Article	IF	CITATIONS
271	Transport number determination by the concentration-cell/open-circuit voltage method for oxides with mixed electronic, ionic and protonic conductivity. Solid State Ionics, 1995, 77, 167-174.	2.7	109
272	Proton conduction in Ca- and Sr-substituted LaPO4. Solid State Ionics, 1995, 77, 240-243.	2.7	170
273	XPS and SEM studies of Ca- and Ni-substituted LaCrO3 after quenching from reducing and oxidizing atmospheres at 800 ŰC. Surface and Interface Analysis, 1994, 22, 275-279.	1.8	6
274	A low-angle grain boundary in iron-doped strontium titanate revealed by transmission electron microscopy. Journal of Materials Science Letters, 1994, 13, 1789-1792.	0.5	1
275	Protons in LaErO3. Solid State Ionics, 1994, 70-71, 305-310.	2.7	42
276	Electrical conductivity and ionic transport number of YSZ and Cr-doped YSZ single crystals at 200–1000°C. Solid State Ionics, 1993, 67, 57-64.	2.7	19
277	Protonic Conduction in Acceptor-Doped Cubic Rare-Earth Sesquioxides. Journal of the American Ceramic Society, 1992, 75, 1176-1181.	3.8	53
278	Impedance spectroscopy studies of electrode-electrolyte systems. Solid State Ionics, 1992, 52, 93-97.	2.7	5
279	Protons in Ca-doped La2O3, Nd2O3 and LaNdO3. Solid State Ionics, 1992, 53-56, 446-452.	2.7	16
280	Electrical conductivity and defect structure of lithiumdoped magnesium oxide. Applied Catalysis, 1991, 71, 89-102.	0.8	19
281	Protonic conductivity in Ca-doped yttria. Solid State Ionics, 1991, 49, 73-77.	2.7	21
282	The electrode system ‗ZrO2: 8Y2O3 investigated by impedence spectroscopy. Solid State Ionics, 1991, 47, 161-167.	2.7	48
283	Liquid phases in Li:MgO as studied by thermoanalytical methods, electron microscopy, and electrical conductivity measurements. Catalysis Today, 1990, 6, 575-586.	4.4	23
284	Hydrogen Defects in Inorganic Solids. Studies in Inorganic Chemistry, 1989, 9, 101-142.	0.2	13
285	Protons in ZrO2; A Search for Effects of Water Vapour on the Electrical Conductivity and M/T Phase Transformation of Undoped ZrO2. , 1989, , 209-218.		3
286	EMF method determination of conductivity contributions from protons and other foreign ions in oxides. Solid State Ionics, 1988, 28-30, 1586-1591.	2.7	113
287	Proton and native-ion conductivities in Y2O3 at high temperatures. Solid State Ionics, 1986, 20, 169-184.	2.7	109
288	Direct-Current Conductivity of Y2O3 as a Function of Water Vapor Pressure. Journal of the American Ceramic Society, 1986, 69, 780-783.	3.8	45

#	Article	IF	CITATIONS
289	Electrical Conductivity of Y2O3 as a Function of Oxygen Partial Pressure in Wet and Dry Atmospheres. Journal of the American Ceramic Society, 1986, 69, 784-789.	3.8	47
290	Electrical Conductivity and Defect Structure of Y2O3as a Function of Water Vapor Pressure. Journal of the American Ceramic Society, 1984, 67, 786-792.	3.8	93